Quality of Service-Driven Overlapping Cooperative NOMA Scheme

Asmaa Amer*, Sahar Hoteit*, Jalel Ben Othman*†
*Université Paris-Saclay, CNRS, CentraleSupélec, Laboratoire des signaux et systèmes, 91190, Gif-sur-Yvette, France
†Université Sorbonne Paris Nord, Paris, France
Emails: {asmaa.amer, sahar.hoteit, jalel.benothman}@centralesupelec.fr

***Abstract*—The rapid growth of connection density drives the next-generation wireless networks into ultra-large-scale systems with massive access demand. Therefore, massive access is crucial in next-generation multiple access design. Although non-orthogonal multiple access (NOMA) enhances user access and quality of service (QoS), NOMA and specifically cooperative NOMA (CNOMA) are limited in the literature by a trade-off between user access (i.e., number of users sharing the resources) from one side and successive interference cancellation (SIC) complexity and interference from the other side. To address this limitation, an overlapping CNOMA (O-CNOMA) scheme is proposed in this study. In multi-user O-CNOMA system, we formulate an optimization problem to maximize the cell-edge users' QoS satisfaction by controlling the overlapping cooperation among cell-center and cell-edge users. We utilize matching theory to address this issue. The proposed scheme's efficiency is confirmed through numerical results. Explicitly, O-CNOMA enables more flexible resource sharing and cooperation between users, outperforming the conventional CNOMA baselines in terms of average throughput, QoS satisfaction and SIC complexity. This makes O-CNOMA a promising scheme for practical implementation in 5G and beyond large-scale systems.**

***Index Terms*—NOMA, Overlapping CNOMA, QoS Satisfaction**

I. Introduction

Cisco predicts that there will be over 75.4 billion connected devices with various applications by 2025 [1]. This propels the next-generation wireless networks, i.e., beyond the fifth-generation (B5G) networks, to be ultra-large-scale systems that must meet the stringent requirements of emergent applications (e.g., augmented reality, intelligent transportation systems, etc.). Consequently, a critical consideration for next-generation multiple access (NGMA) design is the massive user access while guaranteeing the quality of service (QoS) requirements [2]. In contrast to orthogonal multiple access (OMA) techniques, non-orthogonal multiple access (NOMA) is a prominent NGMA technique suited to handle ultra-large-scale B5G networks [2]. In particular, power-domain NOMA enables superposing users' signals over the same time-frequency resources via power-domain multiplexing, using superposition coding (SC) and successive interference cancellation (SIC) at the transmitter and receiver, respectively.

Nevertheless, a NOMA key concern is the receiver's ability to handle the interference resulting from the superposition of multiple users' transmissions over the same resources. Each user, via SIC, decodes the interference of all users with lower channel gains. Consequently, as more users share the same resources, interference and SIC complexity become a concern. Thus, most NOMA literature primarily focuses on the pairing-based scheme, i.e., only two users share the same resources. However, relying on pairing will not be sufficient to meet the massive access demands. Thus, designing large-scale NOMA systems requires rethinking interference and SIC while considering the massive connectivity, which is a fundamental aspect of non-orthogonal access evolution towards 6G networks [2].

Additionally, the integration of cooperative relaying has introduced cooperative NOMA (CNOMA) [3]. CNOMA harnesses SIC and allows strong users to relay data to the weaker users. In [3], a large-scale grouping-based CNOMA is proposed, where the base station (BS) superimposes and transmits the signals of multiple users (i.e., more than two) over the same resources. Each user decodes all weaker users' signals successively before decoding its own, and then forwards the decoded signals to these weaker users. This raises the following concerns: *(1)* multi-stage SIC and additional time slots are required for cooperation, resulting in two extreme-case users: (i) the strongest user with the maximum multiple SIC stages, (ii) the weakest user with the maximum interference level but with reception of multiple cooperation signals, which may be interesting, but opposed with propagated decoding errors and long waiting time before decoding its data relayed successively; this diminished the value of time and power resources used for cooperation; *(2)* low possibility of sufficient received power disparity among users, what prevents SIC success unless sensitive complicated receiver architectures are designed [2, 4]. Due to these concerns, most CNOMA literature adopts the pairing-based CNOMA (P-CNOMA) scheme where only a strong user and a weak user share the resources, and cooperate [5–16]. It is noteworthy that CNOMA holds a promise in large-scale systems with massive user access demand, potentially mitigating weaker users' challenges due to resource tightness and higher interference impact. Therefore, to cope with conventional CNOMA limitations, in this study, an overlapping cooperative non-orthogonal multiple access (O-CNOMA) scheme is proposed. O-CNOMA pursues three goals: *(1) Enabling higher user connectivity under the same resources*; *(2) Improving the cell-edge users' performance*; and *(3) Maintaining a low SIC receiver complexity*. To the best of our knowledge, this is the first work to propose an O-CNOMA scheme overcoming conventional CNOMA limitations.

The rest of the paper is structured as follows. Section II presents the state of the art. Section III, IV, and V define the system model, formulate the problem, and detail the proposed solution, respectively. Section VI presents the numerical results. Section VII concludes the study and provides perspectives.

II. Related works

The CNOMA-based systems have been extensively investigated in the literature [5–16]. The outage probability and throughput in a multiple dedicated half-duplex relays-assisted

ISBN 978-3-903176-63-8 © 2024 IFIP

CNOMA system are derived in [5]. In [6], the authors propose a 3-user half-duplex CNOMA system with a 2-user BS-users transmission phase, where no direct link between the BS and the third user, and a pairing-based cooperative phase. Authors in [7] propose a downlink multi-user NOMA system, where they switch between CNOMA and non-CNOMA modes at cell-center users. Under a similar framework, a CNOMA system with two-way cooperation between cell-center and cell-edge users is enabled in [8]. An RIS-assisted CNOMA scenario is investigated in [9], where RIS assists both the direct BS-users transmission and the strong-weak users cooperative transmission. Apart from users cooperation in [6–9], in [10], in a two-user NOMA system, dedicated relay cooperation for the weak user is compared with RIS-assisted cooperation. Similarly, in [11], a dedicated half-duplex relay connects the BS with the two NOMA users in both scenarios of direct/no-direct link between the BS and two users, where outage probability and bit error rate are analyzed. The authors in [12] investigate a two-user uplink CNOMA system where an adaptive SIC order is proposed. In a multi-user system, the authors in [13] propose a coordinated multipoint assisted CNOMA system, where cell-edge users at the overlapping coverage area of adjacent cells are served by both cells, meanwhile in each cell, pairing-based CNOMA is applied. Similarly, authors in [14–16], adopt pairing-based CNOMA in a multi-user system with underlay D2D communication. Apparently, the aforementioned works focus on pairing-based scenarios. Also, in terms of cooperation, these works studied one cooperation source. Few research works optimizes unconventional resource sharing between NOMA users by proposing partial-NOMA [17], where parts of the user signals are NOMA-superposed, and the others are OMA-transmitted. Moreover, authors in [18] propose an uplink NOMA grouping with user overlap among multiple groups, employing the excess user maximum uplink power in multiple groups to avoid wasting power. These works do not consider the cooperation among NOMA users.

Most research works are limited to pairing-based CNOMA systems to alleviate interference and SIC complexity of large-scale grouping-based CNOMA systems. This is the first work to propose an overlapping cooperative NOMA scheme. The exact contributions of this paper are summarized as follows:

- Proposition of a new overlapping cooperative NOMA scheme with the concept of multiple pairs cooperation, (Fig. 1(a)). We define an O-CNOMA group that consists of several cell-center users and one cell-edge user. Within each O-CNOMA group, each cell-center user forms a CNOMA pair with this cell-edge user. Consequently, the cell-edge user becomes a part of multiple CNOMA pairs, referred to as the overlapping cell-edge user. The overlapping cell-edge user receives relaying from the cell-center users of its corresponding O-CNOMA group.
- Formulation of an optimization problem to maximize the CEUs' QoS satisfaction. It optimizes the cooperation between cell-center users and cell-edge users. A low-complexity matching theory-solution is proposed.
- Comparison of the O-CNOMA scheme with P-CNOMA and grouping-based CNOMA (G-CNOMA) illustrated in Fig.1(b) and Fig. 1(c), respectively. We consider the cell-edge users' average throughput and QoS satisfaction, and cell-center users' SIC complexity as performance metrics.

Our proposed system model is detailed in the next section.

III. System Model

In this study, a downlink single-cell CNOMA-based system is considered with single-antenna BS of power budget P_{BS}. The BS serves U single-antenna users, denoted by

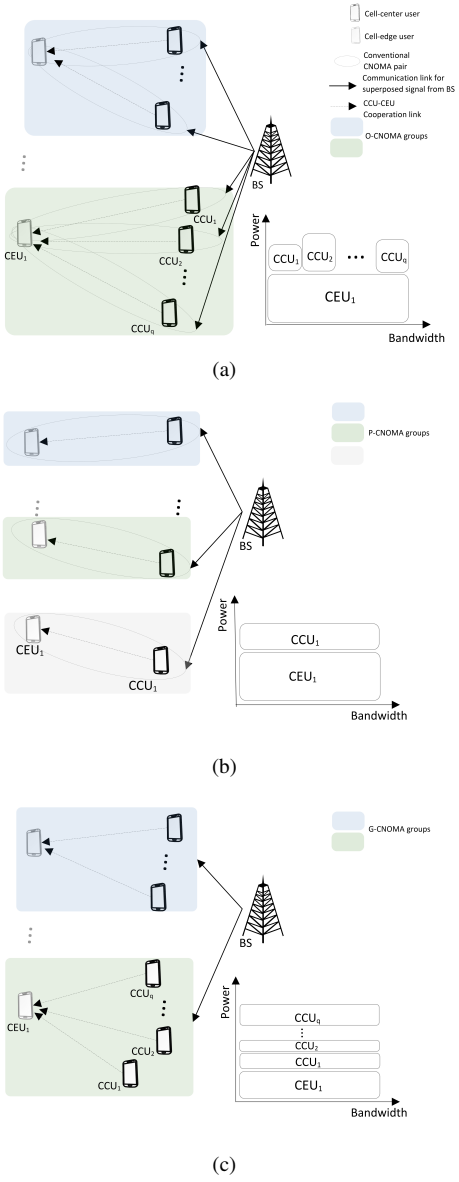

Fig. 1: (a) O-CNOMA, (b) P-CNOMA, (c) G-CNOMA.

$\mathcal{U} = \{1, 2, ..., U\}$. The available bandwidth is divided into a set of resource blocks (RBs) $\mathcal{R} = \{1, 2, ..., |\mathcal{R}|\}$, each with bandwidth B. All communication links are modeled with small- and large-scale fading. Large-scale fading is modeled as path loss $L(d)$, where d is the distance. Thus, the channel gain coefficients are given as $h = gL(d)$, where g captures Rayleigh fading. $\mathbf{h_{a,b}} = \left[h^1_{a,b}, h^2_{a,b}, \ldots, h^{|\mathcal{R}|}_{a,b}\right]$ denotes channel gain coefficients between transmitter a and receiver b, over all RBs $r \in \mathcal{R}$. The perfect knowledge of the channel gain coefficients is assumed. Cell-edge users may suffer from poor channel gains, so CNOMA is enabled to compensate their performance degradation. The system model is depicted in Fig. 1(a) and more details are given in what follows.

Users are classified into cell-center users (CCUs) and cell-edge users (CEUs), denoted by $\mathcal{U}_c$ and $\mathcal{U}_e$, respectively. CCUs and CEUs are assumed to have relatively large and small channel gains to the BS, respectively [3]. Additional details

are elaborated on the users' distribution in Section VI.

We propose an overlapping CNOMA scheme. We define an O-CNOMA group that consists of q CCUs, where $1 \leq q \leq |\mathcal{U}_c|$, and one CEU $v \in \mathcal{U}_e$. Each CCU u receives its signal from the BS over the set of its allocated RBs denoted by $\mathcal{R}_u \subset \mathcal{R}$. Meanwhile, the CEU v receives its BS transmission over the same RBs of each of the q cell-center users. Moreover, given that each of the q CCUs decodes data of v via a one-stage SIC, the CEU v receives q cooperation signals. Both the BS-users transmission and CCUs-CEU cooperation phases, within each O-CNOMA group, are detailed in the following:

- **BS-users transmission:** Each O-CNOMA group is represented as a set of q conventional CNOMA pairs, overlapping at CEU v, given as $\{(u, v), (u', v), (u'', v), \dots\}$. The BS implements SC to superimpose the users' signals of each CNOMA pair, i.e., CCU data and v data. Then, BS transmits the superposed signal over the allocated RBs.
- **CCUs-CEU cooperation:** Exploiting SIC applied at the q CCUs to decode the data of v, each CCU acts as a full-duplex relay to forward the decoded data to v, but it will be affected by self-interference (SI).

The received signals, signal-to-interference-and-noise ratio (SINR), and throughputs are formulated, in what follows.

First, the BS transmits a superposed signal over RB $r \in \mathcal{R}_u$, to the CNOMA pair consisting of CCU u and CEU v, as $x = \sqrt{P_u^r}x_u + \sqrt{P_v^r}x_v$, where x_u, P_u^r, x_v and P_v^r denote the data of u and v and their allocated powers over RB r, respectively. The received signal at the CCU u is given as:

$$y_u^r = h_{BS,u}^r x + h_{u,u}^r \sqrt{P_c^r} x_v + n, \tag{1}$$

where $n \sim \mathcal{CN}(0, BN_0)$ represents the additive white Gaussian noise (AWGN), where N_0 is the noise power spectral density. P_c^r is the cooperating power of CCU u to assist the CEU v; it appears in the self-interference term. The CCU u performs one-stage SIC to decode x_v, subtracts it, then decodes its own data, x_u. Thus the received SINR to decode x_v and x_u at CCU u can be formulated, respectively, as follows:

$$\gamma_{u,v}^r = \frac{P_v^r |h_{BS,u}^r|^2}{P_u^r |h_{BS,u}^r|^2 + P_c^r |h_{u,u}|^2 + BN_0}, \tag{2}$$

$$\gamma_u^r = \frac{P_u^r |h_{BS,u}^r|^2}{P_c^r |h_{u,u}|^2 + BN_0}. \tag{3}$$

We define $\Delta = [\delta_{\mathbf{1}}, \delta_{\mathbf{2}}, \dots]$ with $\delta_{\mathbf{v}} = [\delta_{1,v}, \delta_{2,v}, \dots]^T$, where $\delta_{u,v} \in \{0, 1\}, u \in \mathcal{U}_c, v \in \mathcal{U}_e$ as a binary variable equal to 1 if CEU $v \in \mathcal{U}_e$ is assisted by CCU $u \in \mathcal{U}_c$, and 0 otherwise, such that $\sum_u \delta_{u,v} = q \leq Q$, and $\sum_v \delta_{u,v} = 1$. We denote by Q the maximum number of CNOMA pairs that overlap in CEU v, i.e., the maximum number of CCUs that can assist each CEU v. So, any CEU v receives over RB $r \in \{\bigcup_{u \in \mathcal{U}_c} \mathcal{R}_u | \delta_{u,v} = 1\}$, a BS direct signal and a relayed copy from each CCU u, such that $\delta_{u,v} = 1$. The direct and relayed signals to CEU v over RB r are given in (4) as follows:

$$y_{v,BS}^r = h_{BS,v}^r (\sqrt{P_u^r} x_u + \sqrt{P_v^r} x_v) + h_{u,v}^r \sqrt{P_c^r} x_v + n \tag{4}$$

Assuming that the two signals are fully resolvable at CEU v, they can be co-phased and merged using the maximal ratio combining technique, so the received SINR is given as follows:

$$\gamma_{MRC}^r = \frac{P_c^r |h_{u,v}|^2}{BN_0} + \frac{P_v^r |h_{BS,v}^r|^2}{P_u^r |h_{BS,v}^r|^2 + BN_0}. \tag{5}$$

Therefore, the throughputs of u and v can be given as follows:

$$R_u = \sum\nolimits_{r \in \mathcal{R}_u} Blog_2(1 + \gamma_u^r), \tag{6}$$

$$R_v = \sum\nolimits_{u \in \mathcal{U}_c} \delta_{u,v} \sum\nolimits_{r \in \mathcal{R}_u} Blog_2\big(1 + min(\gamma_{u,v}^r, \gamma_{MRC}^r)\big). \tag{7}$$

The minimum term in (7) is due to the decoding success constraint where SINR of decoding x_v at u should be greater than SINR of decoding x_v at v; thus it is limited by $\gamma_{u,v}$[19].

In the next section, the optimization problem is formulated.

IV. Problem Formulation

Our objective is to enhance the average cell-edge users' QoS satisfaction index. This is achieved by optimizing the cooperation decision between the cell-center users and cell-edge users, i.e., Δ. In the following, we first define the average satisfaction index of CEUs, and then, we formulate our optimization problem along with its constraints.

Based on minimum throughput R_{min}, the users' QoS satisfaction is captured as $b_j = 1$, if $R_j \geq R_{min}$ and $b_j = 0$, otherwise. Therefore, the average CEU QoS satisfaction index is $C_{av} = \frac{\sum_{j \in \mathcal{U}_e} c_j}{|\mathcal{U}_e|}$, where $c_j = (1 - b_j)\frac{R_j}{R_{min}} + b_j, \;\; j \in \mathcal{U}$.

The optimization problem can be formulated as follows:

$$\begin{aligned}
\textbf{P1:} \max_{\Delta} \quad & C_{av}(\Delta) \\
\text{s.t.} \quad & \mathbf{C}_1 : \delta_{u,v} \in \{0, 1\}, \forall u \in \mathcal{U}_c; v \in \mathcal{U}_e, \\
& \mathbf{C}_2 : 1 \leq \sum\nolimits_{u \in \mathcal{U}_c} \delta_{u,v} \leq Q, \quad \forall v \in \mathcal{U}_e, \\
& \mathbf{C}_3 : \sum\nolimits_{v \in \mathcal{U}_e} \delta_{u,v} = 1, \quad \forall u \in \mathcal{U}_c, \\
& \mathbf{C}_4 : \sum\nolimits_{u \in \mathcal{U}_c} P_u + \sum\nolimits_{v \in \mathcal{U}_e} P_v \leq P_{BS}, \\
& \mathbf{C}_5 : \sum\nolimits_{u \in \mathcal{U}_c} |\mathcal{R}_u| \leq |\mathcal{R}|, \\
& \mathbf{C}_6 : P_c \leq P_{c,max}, \\
& \mathbf{C}_7 : P_v^r \geq \delta_{u,v} P_u^r, \;\; \forall u \in \mathcal{U}_c; v \in \mathcal{U}_e; r \in \mathcal{R}
\end{aligned} \tag{8}$$

where $\mathbf{C}_1$ ensures the binary decision, $\mathbf{C}_2$ limits each CEU to share the RBs of at most Q CCUs and be assisted by them, and $\mathbf{C}_3$ limits each CCU to share the RBs with only one CEU and assist it. The constraints $\mathbf{C}_4$ and $\mathbf{C}_5$ ensure the allocated power and RBs are within the BS budget, respectively, while $\mathbf{C}_6$ constrains CCU's cooperating power within its budget, and $\mathbf{C}_7$ ensures the power allocation condition within CNOMA pairs. **P1** is a non-convex problem that introduces computational complexity to solve. Motivated by matching theory potential for practical implementation [20–22], we formulate the problem as a many-to-one matching game, and a low-complexity matching algorithm is proposed in Section V.

V. Proposed Matching-Theory solution

In this section, we aim to solve **P1**. An O-CNOMA group is formed over q overlapping pairs $\{(u_1, v), (u_2, v), \dots, (u_q, v)\}$, where $u \in \mathcal{U}_c$ and $v \in \mathcal{U}_e$, so denote it by the tuple $O = \{v, u_1, u_2, \dots, u_q\}$. We need to determine which CCUs and CEU form each tuple O. The CCU-CEU relationship can be mapped as a many-to-one matching game, where the CCUs and CEUs are the two players' sets. Each CEU v is matched to q CCUs, and each CCU is matched to only one CEU. The matching theory model is presented in what follows:

Definition 1. (*Many-to-one matching* Ψ). A many-to-one matching Ψ is defined as a mapping from $\mathcal{U}$ to $\mathbb{O} = \{O, O', \dots\}$, where $|\mathbb{O}| = |\mathcal{U}_e|$, while satisfying the following:

Algorithm 1: Cooperation matching algorithm

Input : $\mathcal{U}_c$, $\mathcal{U}_e$, Δ
Match CCUs randomly to CEUs, $\Psi \leftarrow \Psi^0$; $\Delta \leftarrow \Delta^0$
repeat
  foreach $i \in \mathcal{U}$ **do**
    if $i \in \mathcal{U}_c$ **then**
      $U_{search} \leftarrow \mathcal{U}_c \backslash \{i' | \psi(i') = \psi(i)\} \cup \phi^{\mathcal{U}_e}$
    else
      $U_{search} \leftarrow \mathcal{U}_e \backslash \{i\}$
    end
    foreach $i' \in \mathcal{U}_{search}$ **do**
      if *(i, i') satisfies the conditions of swap-blocking pair and the constraints* **then**
        i and i' swap their matches,
        $\Psi \leftarrow \Psi_{swap}$
      else
        i and i' do not swap; $\Psi \leftarrow \Psi$
      end
    end
    Update $\phi^{\mathcal{U}_e}$
  end
until *No swap-blocking pair exists*;
Output : $\Delta^{final}, \psi^{final}$

1) $\mid \Psi(u) \mid = 1$ and $\Psi(u) \in \mathcal{U}_e$, $\forall\ u \in \mathcal{U}_c$;
2) $1 \leq \mid \Psi(v) \mid \leq Q$ and $\Psi(v) \subset \mathcal{U}_c$, $\forall v \in \mathcal{U}_e$;
3) $v = \Psi(u) \iff u \in \Psi(v)$, $\forall\ u \in \mathcal{U}_c$, $v \in \mathcal{U}_e$;

Definition 2. (*Utility functions*). The utility function of any user $i \in \mathcal{U}$, under matching Ψ, is defined as $\mathbb{U}_i(\Psi) = c_i$.

Definition 3. (*swap-matching operation*). A swap-matching $\Psi_{swap} \in \{\Psi^{u_1,u_1'}, \Psi^{u_1,\phi^{v'}}, \Psi^{v,v'}\}$ is defined under a swap-operation between: u_1 and u_1', u_1 and $\phi^{v'}$, v or v', respectively:

$$\Psi^{u_1,u_1'} = \{\Psi \backslash \{v, u_1, u_2, \ldots, u_q\}, \{v', u_1', u_2', \ldots, u_{q'}'\}\} \cup \{\{v, u_1', u_2, \ldots, u_q\}, \{v', u_1, u_2', \ldots, u_{q'}'\}\}, \quad (9)$$

such that $\Psi(u_1) = v$, $\Psi(u_1') = v'$, $\Psi^{u_1,u_1'}(u_1) = v'$ and $\Psi^{u_1,u_1'}(u_1') = v$,

$$\Psi^{u_1,\phi^{v'}} = \{\Psi \backslash \{v, u_1, u_2, \ldots, u_q\}, \{v', u_1', u_2', \ldots, u_{q'}'\}\} \cup \{\{v, u_2, \ldots, u_q\}, \{v', u_1', u_2', \ldots, u_{q'}', u_1\}\} \quad (10)$$

such that $\Psi(u_1) = v$, $\Psi(v') = \{u_1', u_2', \ldots, u_{q'}'\}$, and $\phi^{v'} \in \phi^{\mathcal{U}_e}$ denotes an available position at v' to be assisted by more CCUs, where $\phi^{\mathcal{U}_e}$ denotes the available positions at each $v' \in \mathcal{U}_e$ such that $|\Psi(v')| < \mathrm{Q}$. After swap, $\Psi^{u_1,\phi^{v'}}(u_1) = v'$ and $\Psi^{u_1,\phi^{v'}}(v) = \{u_2, \ldots, u_q\}$.

$$\Psi^{v,v'} = \{\Psi \backslash \{v, u_1, u_2, \ldots, u_q\}, \{v', u_1', u_2', \ldots, u_{q'}'\}\} \cup \{\{v', u_1, u_2, \ldots, u_q\}, \{v, u_1', u_2', \ldots, u_{q'}'\}\}, \quad (11)$$

such that $\Psi(v) = \{u_1, u_2, \ldots, u_q\}$, $\Psi(v') = \{u_1', u_2', \ldots, u_{q'}'\}$, $\Psi^{v,v'}(v) = \{u_1', u_2', \ldots, u_{q'}'\}$ and $\Psi^{v,v'}(v') = \{u_1, u_2, \ldots, u_q\}$.

Definition 4. (*(Swap-blocking pair*). (u, u'), (v, v') and $(u, \phi^{v'})$ are swap-blocking pairs (where $u, u' \in \mathcal{U}_c$, $v, v' \in \mathcal{U}_e$ and $\phi^{v'} \in \phi^{\mathcal{U}_e}$) if and only if: $\forall i$, $\mathbb{U}_i(\Psi_{swap}) \geq \mathbb{U}_i(\Psi)$ $\exists i$ such that $\mathbb{U}_i(\Psi_{swap}) > \mathbb{U}_i(\Psi)$, where i is any CCU or CEU that is affected by Ψ_{swap}.

Based on the aforementioned definitions, a matching Ψ is stable if and only if there exist no swap-blocking pairs. A swapping-based overlapping cooperation matching is detailed in Algorithm 1. It initiates with a random matching then searches for swap-blocking pairs. The algorithm runs until no swap-blocking pairs exist. The convergence, stability and complexity of the algorithm are analyzed hereafter:

1) *Convergence:* Given the finite player sets' sizes, i.e., $|\mathcal{U}_c|$ and $|\mathcal{U}_e|$, the swap-blocking pairs and the swap operations are finite. Moreover, any swap operation is approved only if the overall utility (i.e., average satisfaction index C_{av}) increases (**Definition 4**). However, C_{av} is upper-bounded by unity. Thus, the algorithm converges after a finite number of iterations I.

2) *Stability:* The stability is conditioned on the absence of swap-blocking pairs. Assume that a final matching, denoted as ψ^{final}, is not stable. This implies that there is at least one additional swap-blocking pair that leads to another swap operation, resulting in a different final matching different from ψ^{final}. Therefore, ψ^{final} can not be considered truly final. Thus, if the matching is not stable, it is not final, and more iterations are required to reach the final stable matching.

3) *Complexity:* I iterations are required until convergence. While no closed-form of I, but I has been proven to be finite in the convergence analysis. For each iteration, the maximum number of required swap operations is bounded by $|\mathcal{U}_e|^2 + |\mathcal{U}_c|^2 + |\mathcal{U}_c||\mathcal{U}_e|$. Consequently, the computational complexity of the algorithm can be expressed as $\mathcal{O}\big(I\big(|\mathcal{U}_c|^2 + |\mathcal{U}_e|^2 + |\mathcal{U}_c||\mathcal{U}_e|\big)\big)$, indicating a polynomial complexity.

In the next section, the performance of our proposed O-CNOMA scheme is compared to other baselines.

VI. Numerical Results

In this section, the performance of O-CNOMA scheme is evaluated and compared to P-CNOMA and G-CNOMA schemes. We assume an urban microcell environment with a BS and 500 m coverage radius. The CCUs are uniformly distributed from $d_{min} = 10$ m to 20% of the radius, and the CEUs from 85% to 100% of it. The communication channels capture both large- and small-scale fading. For large-scale fading, the BS-CCUs and BS-CEUs channels follow the line-of-sight (LoS) and the non-LoS (NLoS) path loss models, respectively as: $L^{LoS}(d) = -40log(d) - 2log(f) + 4$, and $L^{NLoS}(d) = -36.7log(d) - 26log(f) - 22.7$ [23, 24]. Thus, the BS-CCU and BS-CEU channel gains are given as: $h_{BS,u} = \sqrt{L^{LoS}(d_u)}\left(\sqrt{\left(\frac{K}{1+K}\right)}g'_{BS,u} + \sqrt{\left(\frac{1}{1+K}\right)}g_{BS,u}\right)$, and $h_{BS,v} = \sqrt{L^{NLoS}(d_v)}g_{BS,v}$, respectively . Denote by $K = 3$, the Rician factor, g', the LoS channel, and g, the NLoS channel that follow Rayleigh distribution. The SI channel gain follows a random Gaussian variable with zero mean

Parameter	Symbol	Value
Maximum BS power, CCU power	P_{BS},P_c	38, 10 dBm
Minimal throughput	R_{min}	1 Mbps
Self-interference level	ψ_{SI}	-100dB
Number of RBs and RB Bandwidth	$\|\mathcal{R}\|, B$	25,180KHz
Carrier Frequency	f	2 GHz
AWGN power spectral density	N_0	-174 dBm/Hz

TABLE I: System Parameters

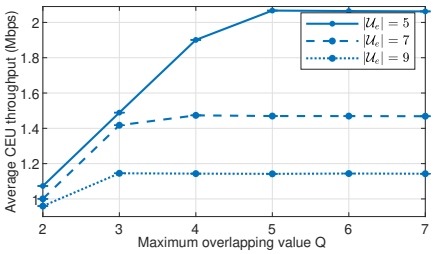

Fig. 2: The average CEU throughput as a function of Q

and variance ψ_{SI}. Unless otherwise stated, Table I lists the system parameters [19, 22]. Numerical results are averaged over 500 user distributions and channel realizations, with 95% confidence intervals. We consider two comparison schemes:

- P-CNOMA: Widely adopted pairing-based CNOMA, where only two users share the same resources (Fig. 1(b)).
- G-CNOMA: Based on CNOMA scheme in [3], with additional required time slots and multiple cooperation phases between each user and weaker users. To be comparable, we modify it to have only one cooperation phase from each CCU to the CEU, simultaneously (Fig. 1(c)).

As performance metrics, we consider the average CEU throughput $R_v^{av} = \frac{\sum_{v \in \mathcal{U}_e} R_v}{|\mathcal{U}_e|}$; the average CEUs QoS satisfaction C_{av}; and CCUs SIC complexity, l_{sic}, i.e., computed as the maximum number of required SIC stages. Evaluating both R_v^{av} and C_{av} is justified as follows. While R_v does not highlight the poorly satisfied CEUs, C_{av} caps the high throughput CEUs with a unit satisfaction thereby masking the highly satisfied CEUs. Thus, C_{av} highlights the dissatisfied-QoS CEUs.

We start in Fig. 2 by studying the impact of the maximum overlapping value Q and the number of CEUs on the average CEUs throughput for a fixed number of CCUs ($|\mathcal{U}_c| = 22$). We can see that a higher R_v^{av} is achieved at a lower number of CEUs, due to less bandwidth and power budget tightness. As Q increases, R_v^{av} increases until a certain value, then it starts to reach a stationary state at a certain value of Q that depends on the system parameters including $|\mathcal{U}_e|$ and $|\mathcal{U}_c|$. At low values of Q, each CEU can be assisted by a lower number of CCUs; what explains the low R_v^{av} at first. After which, a higher number of CCUs assist each CEU, enhancing R_v^{av}.

In Fig. 3, we compare the proposed scheme O-CNOMA, in terms of different performance metrics, with the other two baselines under $|\mathcal{U}_c|$ values, $|\mathcal{U}_e| = 7$ and $Q = 5$. We clearly see from Fig. 3(a) that O-CNOMA outperforms the other baselines. The performance gap becomes more pronounced as $|\mathcal{U}_c|$ increases. For instance, at $|\mathcal{U}_c| = 8$, O-CNOMA achieves approximately an average of 8% and 5% gains, compared to G-CNOMA and P-CNOMA, respectively. This performance gap increases significantly to 102% and 150%, compared to G-CNOMA and P-CNOMA, respectively, at $|\mathcal{U}_c| = 22$.

However, for the CEUs satisfaction index in Fig. 3(b), slightly different observation can be noted. When the number of CCUs is low (i.e., comparable to the number of CEUs), O-CNOMA behavior is similar to P-CNOMA. As $|\mathcal{U}_c|$ increases, O-CNOMA sees a slight decline in response to more CCUs accessing the network (i.e., sharing BS power budget); however, this decline is slower for P-CNOMA. This can be justified as what follows. In P-CNOMA, the increased CCUs are allocated exclusive resources (i.e., not shared with CEUs), so with less power allocation need; this reduces the power tightness compared to O-CNOMA. As $|\mathcal{U}_c|$ continues increasing, in P-CNOMA, more CCUs are allocated exclusive resources, leading to more tightness on bandwidth reflected as a more severe decline in R_v^{av}. Meanwhile, in O-CNOMA, as $|\mathcal{U}_c|$ continues increasing, the overlapping value of each CEU increases, which compensates for the decline caused by the power tightness. For instance, with 22 CCUs, O-CNOMA can achieve an average of 63% and 43% gain in C_{av}, compared to P-CNOMA and G-CNOMA, respectively, while ensuring the same number of accessed users. Therefore,the performance gap between our proposed scheme and the other baselines becomes clearer as $|\mathcal{U}_c|$ increases. The reason is as follows. The decline in the performance of P-CNOMA with the increase in $|\mathcal{U}_c|$ is due to the allocation of exclusive resource blocks to certain CCUs without being shared with other users, hence leading to bandwidth tightness. Also, for G-CNOMA, the higher $|\mathcal{U}_c|$, the larger the conventional CNOMA group size, which yields more significant interference levels at the CCUs, lowering their decoding performance and the relayed data quality as well. On the contrary, despite bandwidth and power tightness, O-CNOMA's performance is approximately constant. This is due to the increase of the overlapping value of CEUs, i.e., more CCUs are relaying each CEU, and while there is no co-channel interference between CCUs in contrast to G-CNOMA. These performance gaps underscore the scalability and effectiveness of our solution in denser scenarios.

Regarding CCUs SIC complexity, we can see in Fig. 3(c), a one-stage SIC complexity. This complexity reduction compared to G-CNOMA is more pronounced as $|\mathcal{U}_c|$ increases.

Overall, the numerical results show that O-CNOMA bridges the conventional P-CNOMA and G-CNOMA, overcomes their defects, and reaps their gains. Compared to P-CNOMA, i.e., restricted to only two users per the same resources, O-CNOMA overcomes its resource utilization inefficiency while maintaining its low SIC complexity. While compared to G-CNOMA, O-CNOMA overcomes its high interference and SIC complexity and achieves its gain of multiple users per the same resources, and with more flexible resource sharing between CEUs and CCUs. Furthermore, from a practical perspective, the SIC complexity reduction supports practical NOMA application, particularly for the energy and computing-constrained users and those requiring short-packet transmission.

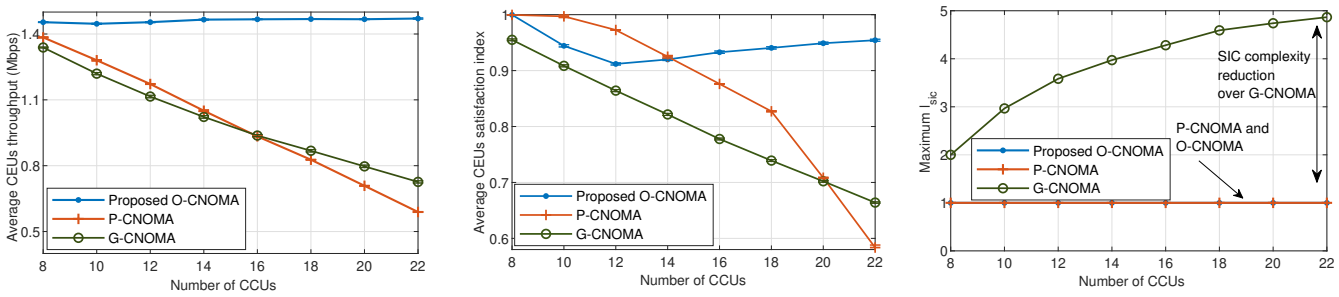

(a) Average CEUs throughput (b) Average CEUs QoS satisfaction index (c) Maximum CCUs SIC complexity

Fig. 3: Comparison of O-CNOMA with P-CNOMA and G-CNOMA for different performance metrics

VII. Conclusion

In this paper, a new overlapping CNOMA scheme has been proposed and compared to two baselines, P-CNOMA and G-CNOMA. P-CNOMA scheme minimizes interference and SIC complexity but at the cost of resource utilization efficiency, while extending it to G-CNOMA scheme boosts resource utilization efficiency, but increases the interference and SIC complexity. O-CNOMA bridges both schemes, enabling multiple CCUs, which are allocated orthogonal resources among each other, to share them with a CEU and assist it, making a CEU overlap among multiple CNOMA pairs. An optimization problem have been formulated to maximize the cell-edge users' QoS satisfaction by controlling the cooperation between CCUs and CEUs. Numerical results have shown the superiority of our O-CNOMA scheme over the conventional schemes in terms of cell-edge users' performance and cell-center users' SIC complexity. As a future work, we aim to provide an adaptable O-CNOMA scheme for broader communication scenarios.

References

[1] Xiaoming Chen et al. "Massive access for 5G and beyond". *IEEE J. Sel. Areas Commun.* 39.3 (2020), 615–637.

[2] Yuanwei Liu et al. "Developing NOMA to next generation multiple access: Future vision and research opportunities". *IEEE Wirel. Commun.* 29.6 (2022), 120–127.

[3] Zhiguo Ding et al. "Cooperative non-orthogonal multiple access in 5G systems". *IEEE Commun. Lett.* 19.8 (2015), 1462–1465.

[4] Valeri Kontorovich. "Comments on SIC design for SISO NOMA systems over Doubly selective channels". *IEEE Open J. Veh. Technol.* 3 (2022), 111–119.

[5] Jeong Seon Yeom et al. "Spectrally efficient uplink cooperative NOMA with joint decoding for relay-assisted IoT networks". *IEEE Internet Things J.* 10.1 (2022), 210–223.

[6] Yao Xu et al. "Adaptive aggregate transmission for device-to-multi-device aided cooperative NOMA networks". *IEEE J. Sel. Areas Commun.* 40.4 (2022), 1355–1370.

[7] Yuan Ren et al. "Incremental Relay Inspired Mode Selection for SWIPT-Enabled NOMA Systems with Imperfect SIC and Random User Locations". In: *2023 IEEE/CIC International Conference on Communications in China (ICCC Workshops)*. IEEE. 2023, pp. 1–6.

[8] Yuan Ren et al. "Impartial Cooperation in SWIPT-Assisted NOMA Systems with Random User Distribution". *IEEE Trans. Veh. Technol.* (2023).

[9] Juanjuan Ren et al. "Ris-assisted cooperative NOMA with SWIPT". *IEEE Wirel. Commun. Lett.* 12.3 (2022), 446–450.

[10] Mingxing Wang et al. "On the achievable capacity of cooperative NOMA networks: RIS or relay?" *IEEE Wirel. Commun. Lett.* 11.8 (2022), 1624–1628.

[11] Safia Beddiaf et al. "A unified performance analysis of cooperative NOMA with practical constraints: hardware impairment, imperfect SIC and CSI". *IEEE Access* 10 (2022), 132931–132948.

[12] Mohamed Elhattab et al. "Power allocation optimization and decoding order selection in uplink C-NOMA networks". *IEEE Commun. Lett.* 27.1 (2022), 352–356.

[13] Mohamed Elhattab et al. "Joint clustering and power allocation in coordinated multipoint assisted C-NOMA cellular networks". *IEEE Trans. Commun.* 70.5 (2022), 3483–3498.

[14] Asmaa Amer et al. "Resource allocation for downlink full-duplex cooperative NOMA-based cellular system with imperfect SI cancellation and underlaying D2D communications". *Sensors* 21.8 (2021), 2768.

[15] Asmaa Amer et al. "Resource allocation for enabled-network-slicing in cooperative NOMA-based systems with underlay D2D communications". In: *ICC 2023-IEEE International Conference on Communications*. IEEE. 2023, pp. 1344–1349.

[16] Asmaa Amer et al. "Throughput maximization in multi-slice cooperative NOMA-based system with underlay D2D communications". *Comput. Commun.* 217 (2024), 134–151.

[17] Beomju Kim et al. "Partial non-orthogonal multiple access (P-NOMA)". *IEEE Wirel. Commun. Lett.* 8.5 (2019), 1377–1380.

[18] Weichao Chen et al. "Generalized user grouping in NOMA based on overlapping coalition formation game". *IEEE J. Select. Areas Commun.* 39.4 (2020), 969–981.

[19] Ali Muhammad et al. "Optimizing Age of Information in RIS-Empowered Uplink Cooperative NOMA Networks". *IEEE Trans. Net. and Service Manag* (2023), 1–1.

[20] Joseph Doumit et al. "AoI Minimization in Mixed Traffic Full-Duplex Uncoordinated Communication Systems With NOMA". *IEEE Internet Things J.* 11.2 (2024), 2830–2841.

[21] Kaidi Wang et al. "A Rate-Splitting Empowered NOMA Network: Power Allocation and User Pairing". *IEEE Trans. Veh. Technol.* (2023).

[22] Yerra Prathyusha et al. "Resource Allocations for Coexisting eMBB and URLLC Services in Multi-UAV Aided Communication Networks for Cellular Offloading". *IEEE Trans. Veh. Technol.* (2023).

[23] Sadayuki Abeta. "Evolved universal terrestrial radio access (eutra); further advancements for e-utra physical layer aspects". *Rep. 3gpp TR 36.814 V9* (2015).

[24] Xu X et al. "Cluster-Free NOMA Communications Toward Next Generation Multiple Access". *IEEE Trans. on Commun.* 71.4, 2184–2200, 2023.